Antarctic Science 16 (2): 133–142 (2004) © Antarctic Science Ltd Printed in the UK DOI: 10.1017/S0954102004001968

Coupling mixing and photophysiological response of Antarctic plankton: a Lagrangian approach

DANIELA CIANELLI[1,2], MAURIZIO RIBERA D'ALCALÀ[2], VINCENZO SAGGIOMO[2] and ENRICO ZAMBIANCHI[1]

[1]*Università degli Studi di Napoli "Parthenope", Via De Gasperi 5, 80133 Napoli, Italy*
[2]*Stazione Zoologica "Anton Dohrn", Villa Comunale, 80121 Napoli, Italy*

Abstract: An individual-based model is presented which describes the spatial and temporal evolution of phytoplankton growth in terms of a Lagrangian ensemble of cells affected by various physical and biological forcing factors. The motion of cells develops according to a turbulent velocity field which simulates the Antarctic mixed layer during the summer. The cell growth is a function of the irradiance regime, nutrient availability and the vertical position of the individual with respect to the other cells (in order to evaluate the self-shading effect). The values of photosynthetic parameters used to simulate the photophysiological response of the organisms are derived from measurements collected in the Ross Sea. In contrast to previous individual-based descriptions, all the physical and biological processes involved are explicitly reproduced in their dynamical features. Coupling different mixing levels with photoacclimation strategies leads to a wide range of photophysiological responses which underline the role of individual physiological histories in determining the growth of the population as a whole. Simulated photosynthetic parameters, chlorophyll *a* concentrations and integrated primary production correspond closely to *in situ* data and confirm that photoacclimation to low irradiance and strong mixing regimes may be considered as crucial factors in the photosynthetic performance of Antarctic phytoplankton.

Received 21 May 2003, accepted 10 December 2003

Key words: individual-based modelling, mixed layer depth, photoacclimation, photoinhibition, phytoplankton

Introduction

During the last decade plankton dynamics in the Southern Ocean have been the focus of several studies. The particular characteristics of this area related to the low latitudes (e.g. the seasonal cycle of solar irradiance and ice together with the strong wind field), have been considered as the factors controlling primary productivity in the Southern Ocean. The high variability in the irradiance experienced by the cells, caused by the frequent vertical displacements in the water column induced by wind mixing and convection, has been frequently considered in particular since this is certainly to induce a biological response from organisms (Strutton *et al.* 2000, Figueiras *et al*. 1999).

There is strong evidence suggesting that the photosynthetic parameters most usually monitored, namely α_{Chl} (Chl *a*-specific initial slope of the P–E curve) and P^B_{max} (the maximum photosynthetic rate), which should directly reflect a response to the specific irradiance regime, generally lie at the lower end of the values displayed by unicellular marine autotrophs (α_{Chl} = 0.024–0.13 mg C·(mg Chl *a*)$^{-1}$·h^{-1} (µmol photons m^{-2} s^{-1})$^{-1}$; P^B_{max} = 0.5–2 mg C (mg Chl *a*)$^{-1}$·h^{-1}; see Table I) with a resulting E_k, the light saturation parameter, of 8–100 µmol photons·m^{-2}·s^{-1} (see Saggiomo *et al.* 2002). This suggests an acclimation to low average irradiance, which in turn would be consistent with a significant vertical movement of the cells. However, low values of P^B_{max} might also be related to the low temperature of Antarctic waters (Neori & Holm-Hansen 1982, Tilzer & Dubinsky 1987, Sakshaug *et al.* 1991), which rarely exceeds 2°C.

Mortain-Bertrand (1989) observed enhanced growth of Antarctic phytoplankters in a highly fluctuating irradiance field (2:2 vs. 12:12 photoperiod), but reported the absence of photoinhibition. However, low values of E_k might occur in conjunction with photoinhibition, which would produce a negative effect on primary production in non-turbulent conditions. Indeed, evidence for both processes (photolimitation and photoinhibition) is contradictory (Sakshaug & Holm-Hansen 1986) while the extent to which light availability is a key factor in controlling plankton growth in the Southern Ocean remains an open question (see also Nelson & Smith 1991, Saggiomo *et al.* 2000).

In order to explore the role of light dependent processes in

Table I. Photosynthetic parameters measured in the Ross Sea during the summer 1996 at three different mixed layer depths (Saggiomo *et al.* 2002).

Mixed layer depth		α_{Chl}	P^B_{max}
0–20 m	min	0.039	1.13
	max	0.132	2.83
	std	0.024	0.46
20–75 m	min	0.024	0.77
	max	0.119	1.36
	std	0.020	0.68
>75 m	min	0.030	0.72
	max	0.123	2.83
	std	0.023	0.39

phytoplankton growth and the possible constraints caused by acclimation, we implemented a 1D Individual Based Model (hereafter referred to as IBM), which mimics several of the key processes related to light variability in the water column. The IBMs consider populations to be composed of a large number of organisms, with explicit rules determining individual physiology and interactions with the environment. In order to represent the realistic dynamics of a phytoplankton population with an IBM, a significant number of cells need to be simulated. One method is based on the assumption that the basic unit of an IBM represents more than one individual. Through this Lagrangian approach (Woods & Onken 1982), identical individuals born at same time are grouped into one unit (referred to as 'particle'). Using a Lagrangian description, the environmental constraint influencing individuals as they move in the water column can be taken into account and the growth of a phytoplankton population can be understood in terms of the unique temporal and spatial history of the individual particle.

The Lagrangian approach to the study of plankton behaviour in the water column was first introduced 25 years ago (Marra 1978, Falkowski & Wirick 1981), but it was only after the work by Woods & Onken (1982) and Wolf & Woods (1988) that it received wider recognition. Several additional contributions subsequently appeared in the literature addressing specific aspects of phytoplankton physiology in a rapidly changing irradiance field (Yamazaki & Kamykowski 1990, Lizon *et al.* 1998). Lande & Lewis (1989) questioned the rationale for using the time-consuming Lagrangian approach as opposed to the traditional Eulerian one, while a recent attempt to overcome the limit imposed by handling average quantities within an Eulerian framework has been proposed by Janowitz & Kamykowski (1999). However, since physiological responses interact in each single organism in a non-linear fashion (e.g. Cullen & Lewis 1988) and since extreme 'behaviours' may often become the critical ones, individual-based modelling may prove to be the most suitable tool for exploring the interaction between organisms and the environment or between various organisms.

Despite the remarkable role in introducing the individual-based approach to simulating phytoplankton growth, the time dependence of biomass and chemical content of the cells has not been described in terms of their dynamical traits in the previous models. As a consequence, the physiological complexity of the single organisms in response to variable environmental signals was not adequately reproduced. Our treatment of phytoplankton physiology is more detailed and explicitly takes into account the dynamics of organic carbon (C) and chlorophyll *a* (Chl *a*) along with the vertical structure of the water column. The acclimation is the result of the adjustment of single organism physiology which occurs when environmental conditions vary. The complexity of phytoplankton physiology is well represented by simulating the rates of change of the biomass variables (C and Chl *a*). The model presented also allows a sensitivity analysis on relevant quantities to be conducted.

Focusing on the specific issue of the effect of light variability in the mixed layer, we carried out simulations in a nutrient-replete, iron-replete environment, which reproduces the conditions frequently observed in coastal areas (Martin *et al.* 1990) or at the onset of the growth season in Antarctica. It is worth noting that the model is designed to take account of additional physiological factors, such as temperature, macronutrient and iron limitation.

The model

The physical environment

Given the extremely limited capability of autonomous motion possessed by planktonic organisms, their trajectories may be modelled as if they were passive particles. The description of passive tracer transport can employ either Lagrangian or Eulerian terms (e.g. Csanady 1973). In this work, the behaviour of organisms or their aggregates is described in Lagrangian terms; however, it is worth emphasizing that the consistency of the Lagrangian description is only guaranteed when an *ensemble* of simulations (Young *et al.* 2001) is taken into account. The description of Lagrangian motion in a turbulent field - as is the case here, where the presence of turbulence is considered the only factor causing the organism displacement - is normally done through stochastic models for particle motion (e.g. Chandrasekhar 1943), where the stochastic portion accounts for the randomness of the turbulent field.

In the last decade autoregressive models of different orders have been developed which mimic particle motion in the ocean. In particular, Markovian processes for the displacement, velocity and acceleration have been recently applied to oceanographic situations (Zambianchi & Griffa 1994, Griffa 1996, Bauer *et al.* 1998, Berloff & McWilliams 2002). In the present work, however, we will use the simplest stochastic model, a random walk which is Markovian in terms of displacement (i.e. in which the particle position is a process whose conditional probability density at a certain time depends solely on its value at the previous time step). As the particle/organism moves through the water column, it receives a random impulse at each time step due to the action of the incoherent turbulent field, and "loses memory" of its previous turbulent momentum (see Zambianchi & Griffa 1994). In Eulerian terms this corresponds to the standard diffusion equation, in which the subgrid turbulent processes are parameterized by eddy diffusivity.

A crucial point in the selection and utilization of Lagrangian models concerns the possibility of generalizing them in the case of inhomogeneous turbulence, which is

https://doi.org/10.1017/S0954102004001968 Published online by Cambridge University Press

particularly relevant in the case of simulations in the vertical, where the eddy diffusivity coefficient is expected to be characterized by at least two different values corresponding to the surface mixed layer and the deep portion of the water column. When the turbulent parameters are vertically dependent, trajectories show a tendency to concentrate in regions of relatively low diffusivity (e.g. van Dop *et al.* 1985). This violates continuity and leads to physically impossible situations.

In this paper we use the scheme proposed by Visser (1997), based in turn on the work by Hunter *et al*. (1993), who introduces an additional component directed up the diffusivity gradient which balances the tendency to have high particle concentrations in lower variance regions.

For each time step (180 s) the organisms move in the 100 m water column with a vertical resolution of 1 m, and the vertical displacement (*dz*) of a single particle is computed as:

$$dz = K_z^{'}(z)dt + r\sqrt{2k_z dt} \tag{1}$$

where

$$K_z^{'}(z) = \frac{\delta k_z}{\delta z} \tag{2}$$

is the vertical gradient of diffusivity, *r* represents a random process which follows a normal distribution with a mean of zero and a standard deviation of $(2\ k_z\ \Delta t)^{1/2}$ and

$$k_z = K_z(z + \tfrac{1}{2}K_z^{'}(z)dt) \tag{3}$$

is the non-random component, introduced on the basis of the "well-mixed" condition of the particles according to criteria stated by Thomson (1987), which "advects" the particles from areas of low diffusivity to areas of high diffusivity and sets the conditions under which models produce a realistic spatial particle distribution. A reflection boundary condition is imposed at the sea surface (z = 0 m).

The irradiance (*E*) profile in the water column is evaluated as:

$$E = E_0 e^{-K_D z} \tag{4}$$

where K_D is the total light attenuation coefficient and E_0, the irradiance incident on the sea surface, is a function of the latitude φ, the sun declination δ (held constant for short-term simulations), the time t and the irradiance at noon, set at 1500 µmol photons $\cdot m^{-2} \cdot s^{-1}$ (Lazzara *et al*. 2000, Saggiomo *et al.* 2002):

$$E_0 = E_{noon}(\sin\varphi\cos\delta - \cos\varphi\cos\delta\cos\frac{t\pi}{12}) \tag{5}$$

The parameterization of the light history of each particle also accounts for the self-shading effect due to the cells being located at different depths in the water column.

In Eq. 4 $K_D = K_W + K_{Chl}$ so that at each time step the attenuation coefficient K_D is computed as the sum of two components: K_W due to the medium and dissolved

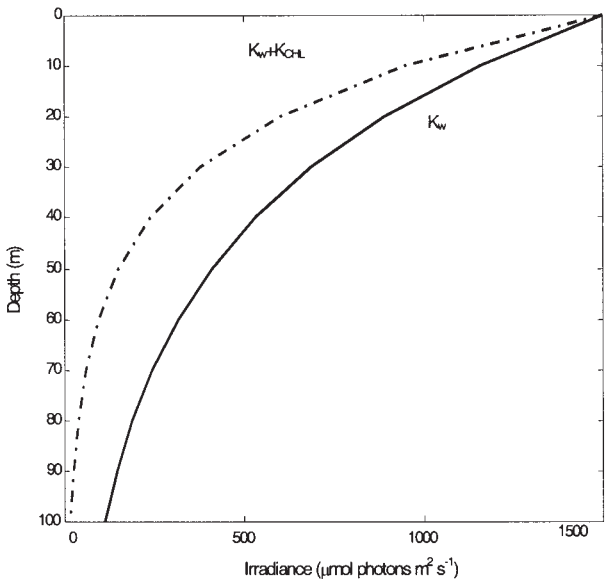

Fig. 1 The irradiance attenuation in the water column as dependent on the medium and presence of dissolved substances (K_w) and on the Chl *a* (K_{Chl}) concentration.

Table II. Variables and parameters used in the model.

Variable	Description	Units
K_z	Vertical diffusivity	$m^2 \cdot s^{-1}$
r	Random process	dimensionless
E	Incident scalar irradiance	µmol photons $\cdot m^{-2} \cdot s^{-1}$
E_0	Irradiance on the sea surface	µmol photons $\cdot m^{-2} \cdot s^{-1}$
E_{noon}	Irradiance at noon	µmol photons $\cdot m^{-2} \cdot s^{-1}$
φ	Latitude	degrees
δ	Sun declination	degrees
K_D	Total light attenuation coefficient	m^{-1}
K_W	Light attenuation coefficient due to the medium and dissolved substances	m^{-1}
K_{Chl}	Light attenuation coefficient due to the Chl *a* distribution	m^{-1}
P	Carbon specific photosynthetic rate	d^{-1}
P_m	Maximum photosynthetic rate	d^{-1}
α_{Chl}	Chl *a*-specific initial slope of the P– E curve	mg C·(mg Chl*a*)$^{-1}$·h^{-1} (µmol photons m^{-2} s^{-1})$^{-1}$
θ_c	Chlorophyll to Carbon ratio	mg Chl *a* · (mg C)$^{-1}$
C	Phytoplankton carbon	mg C m^{-3}
R^C	Respiration rate	d^{-1}
ζ	Cost of biosynthesis	mg C · (mg N)$^{-1}$
V_n	Nitrate uptake rate	mgN · (mg C)$^{-1}$·d^{-1}
Chl	Chlorophyll *a*	mg Chl m^{-3}
ρ_{Chl}	Regulation term for the Chl *a* synthesis	dimensionless
R^{Chl}	Chl *a* degradation rate	d^{-1}
Q	Constant Nitrogen to Carbon ratio	mg N · (mg C)$^{-1}$
ϑ_{Inhib}	Relative concentration of D1 protein	dimensionless
k_d	Damage constant of D1 protein	dimensionless
σ_{PSII}	Optical absorption cross section of Phototosystem II	m^2 · (µmol photons)$^{-1}$
k_r	Recovery rate constant of D1 protein	s^{-1}
n	Concentration of photosynthetic units	mg C · (mg Chl)$^{-1}$
t^{-1}	Minimum turnover time for photon in Photosystem II	s

https://doi.org/10.1017/S0954102004001968 Published online by Cambridge University Press

substances, and K_{Chl} due to the chlorophyll distribution, which varies with time and depth (self-shading effect) (Fig. 1).

Cell response to light (photoadaptation and photoinhibition)

Based on Geider *et al.* (1998), the phytoplankton acclimation to light variability is represented by the Chl:C ratio. The equations solved by the model are (see Table II for an explanation of the symbols used):

$$P = P_m\left[1-\exp\left(-\frac{\alpha_{Chl}E\theta_c}{P_m}\right)\right] \tag{6}$$

$$\theta_c = \frac{Chl}{C} \tag{7}$$

$$\frac{1}{C}\frac{dC}{dt} = P - R^c - \varsigma V_n \tag{8}$$

$$\frac{1}{Chl}\frac{dChl}{dt} = \frac{\rho_{Chl}V_n}{\theta_c} - R^{Chl} \tag{9}$$

$$\rho_{Chl} = \frac{P}{\alpha_{Chl}E\theta_c} \tag{10}$$

$$V_n = P\frac{Q}{1+\varsigma Q} \tag{11}$$

Equation 6 is the classic saturation curve for primary production (Geider *et al.* 1997), and is normalized to carbon. The photosynthetic rate P depends explicitly on the Chl:C ratio (θ_c) and the rate of irradiance absorption is thus proportional to the Chl content of the cell.

The specific rates of variation of C and Chl per cell (Eqs 8 & 9) include consumption through respiration (R^C, R^{Chl}). In addition, the specific rate of increase of C competes with nitrogen uptake (V_n), whereas the specific rate of increase of Chl is inversely proportional to θ_c, and directly proportional to nitrogen uptake and to ρ_{Chl}, a regulating term of Chl *a* synthesis which in turn depends on irradiance (E), photosynthetic efficiency (α_{Chl}), θ_c and P. Q is the nitrogen-to-carbon ratio which, as stated above, is kept constant during the simulations (balanced growth).

One of the aims of this version of the model was to evaluate photoinhibition with respect to irradiance as one of the critical factors for phytoplankton growth. In order to introduce the time dependence of photoinhibition and recovery, we explicitly considered the kinetics of this process. Very few attempts at modelling photoinhibition are reported in the literature (although see Behrenfeld *et al.* 1998, Han *et al.* 2000, Marshall *et al.* 2000).

There is general consensus that damage to the D1 protein of photosystem II (PSII) is responsible for instigating the photoinhibition process. In this paper we use the equations of Han *et al.* (2000), which are easy to parameterize using experimental data. Our depiction of photoinhibition is realistic in terms of the impact on the photosynthetic performance though probably not in terms of the biophysical mechanisms by which it is regulated. The extent of photoinhibition depends on both the damage and the recovery rates of the D1 protein as:

$$\frac{d\vartheta_{Inhib}}{dt} = -k_d\sigma_{PSII}E\vartheta_{Inhib} + k_r\left(1-\vartheta_{Inhib}\right) \tag{12}$$

where ϑ_{Inhib} is the relative concentration of D1 protein, and k_d and k_r are the damage constant and the recovery rate constant of D1 protein respectively. The Chl *a* normalized maximum production P_m can be expressed in terms of n/τ where n is the concentration of photosynthetic units and τ is the minimum turnover time of electron transfer (Sakshaug *et al.* 1997). Thus we may compute P_m by means of the photoinhibition proxy ϑ_{Inhib} and the photoadaptation proxy θ_c, assuming that any variations in the n/τ ratio are predictable:

$$P_m = \frac{n}{\tau}\vartheta_{Inhib}\theta_c \tag{13}$$

In constant light ϑ_{Inhib} converges to a steady value expressed as:

$$\vartheta_{Inhib} = \frac{k_r}{k_r + k_d\sigma_{PSII}E} \tag{14}$$

which allows an estimate of the ratio between k_r and k_d, given a measured change of productivity with irradiance.

Realistic values of the parameters α_{Chl}, k_d, k_r, σ_{PSII}, n, τ were obtained, utilizing the expressions of Sakshaug *et al.*

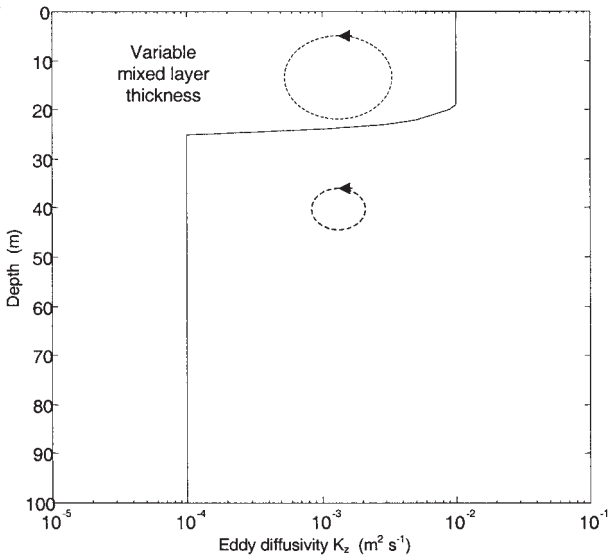

Fig. 2. An ideal eddy diffusivity profile corresponding to the surface mixed layer and to the deep portion of the water column.

https://doi.org/10.1017/S0954102004001968 Published online by Cambridge University Press

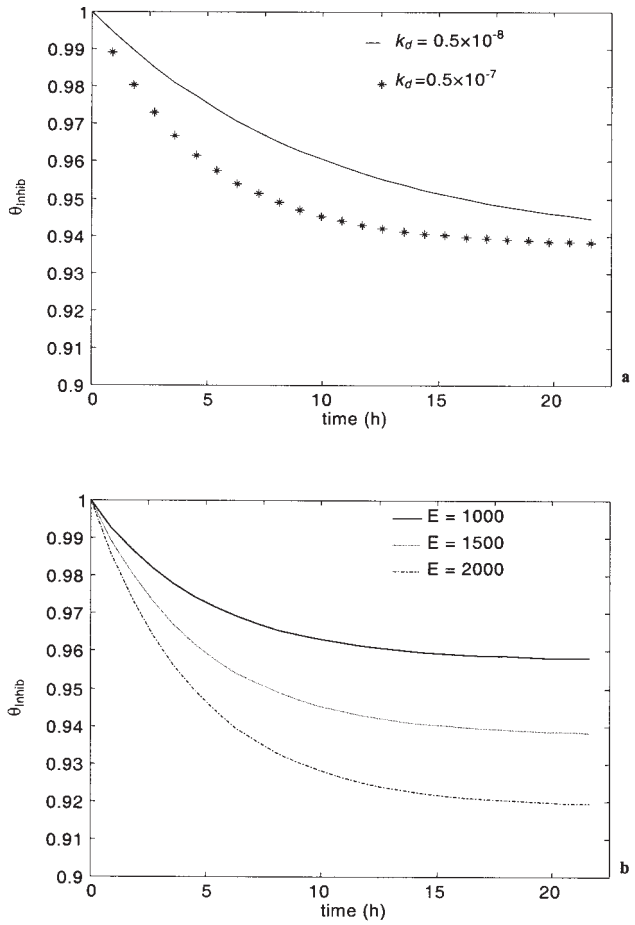

Fig. 3. The time course of photoinhibition under constant light intensity, **a.** at irradiance of 1500 µmol photons·m^{-2}·s^{-1}, with different damage constant of D1 protein $k_d = 0.5 \times 10^{-8}, 0.5 \times 10^{-7}$, **b.** at three irradiance levels corresponding to 1000, 1500, 2000 µmol photons·m^2·s^{-1} with a damage constant of D1 protein set as $k_d = 0.5 \times 10^{-8}$.

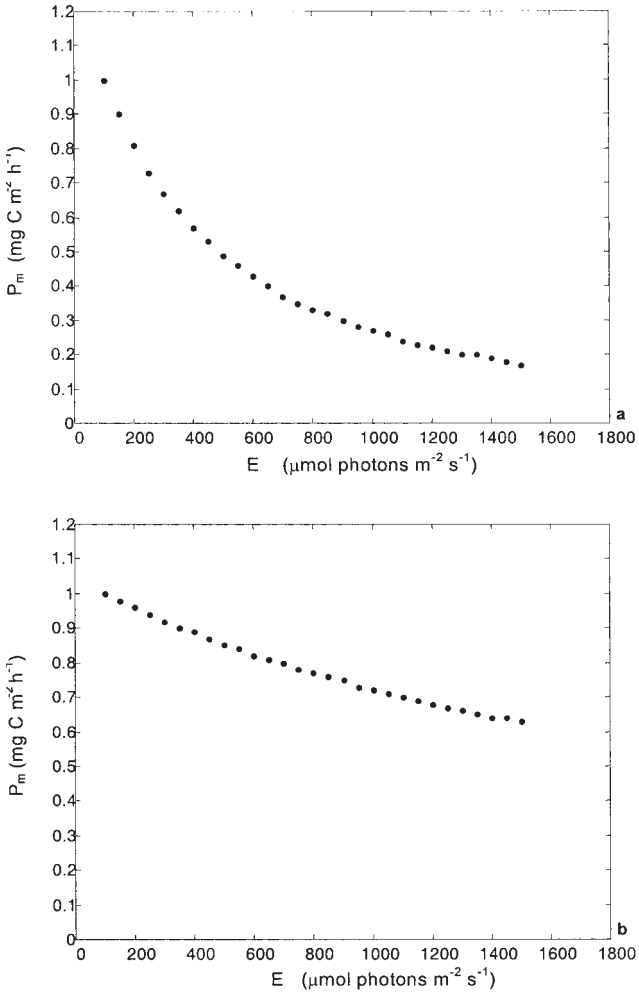

Fig. 4. Variability of P_m (the Chl *a* normalized maximum production) versus E (irradiance) as induced by the two photoadaptative strategies: **a.** Mode 1: P_m is affected only by changes in ϑ_{Inhib}. **b.** Mode 2: P_m decreases proportionally to both θ_C and ϑ_{Inhib}.

(1997), from a number of P–E curves of Antarctic phytoplankton (Saggiomo *et al*. 2002), gathered during a summer cruise in the Ross Sea.

In order to determine the role of mixing in generating differences in the physiological responses of single organisms, we performed a number of ensemble simulations (each one consisting of 50 computations) with different mixed layer depths and two values for the vertical eddy diffusivity (k_z = 10^{-4} – 10^{-2} m^2·s^{-1}), representing the surface mixed layer and the subsurface one respectively (Fig. 2). We started our simulations with 500 particles (each particle represents a cluster of cells designed to reproduce realistic *in situ* concentrations) randomly released from the surface and uniformly distributed.

Results

As a control test we firstly simulated the dynamics of ϑ_{Inhib} for 24 h under constant irradiance and with two constant damage levels in order to check the steady state assumption. Figure 3a shows that for constant irradiance, the kinetic of photoinhibition slows down for decreasing values of k_d and that the steady state is reached in less than two hours. Moreover, the higher the irradiance, the faster are the kinetics of photoinhibition (Fig. 3b).

The photosynthetic activity of the cells depends on the value of n/τ ratio (eq. 13). We derived both parameters from experimental data, assuming no change during incubations, and the data directly reflect the photoacclimation responses of the algae. Since one of our objectives was to analyse the role of the surface mixing in shaping the photophysiological states of organisms with realistic physiology, we let the n/τ ratio change in the two different canonical ways frequently observed in marine algae (e.g. Falkowski & Raven 1997). The first one (Mode 1 in the following) consists of the change in the absolute number of active photosynthetic

https://doi.org/10.1017/S0954102004001968 Published online by Cambridge University Press

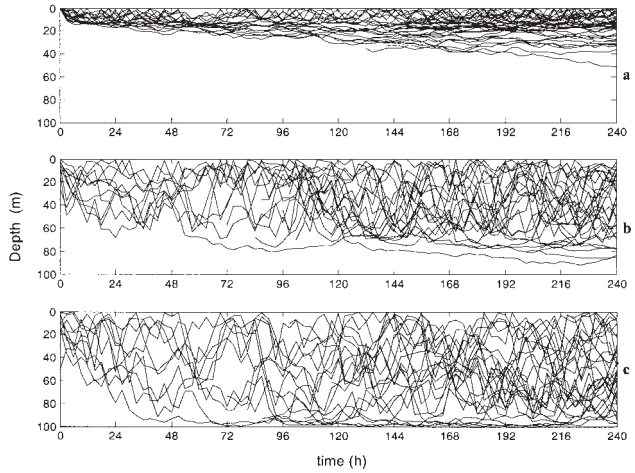

Fig. 5. The trajectories followed by selected particles with a mixed layer depth set as: **a.** 3 m, **b.** 55 m, and **c.** 90 m. The vertical eddy diffusivity ranges from $k_z = 10^{-2}$ m^2 s^{-1} in the surface layer to $k_z = 10^{-4}$ m^2 s^{-1} at depth.

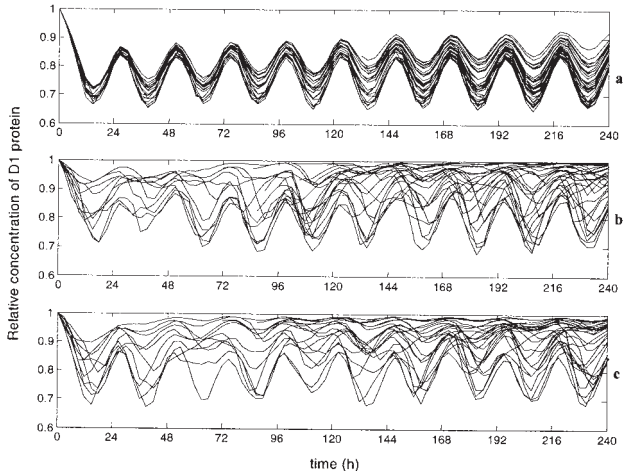

Fig. 7. The relative concentration of D1 protein in the PSII determines the dynamics of the photoinhibition process. The physiological responses of selected particles depends on the mixed layer depth. **a.** 3 m, **b.** 55 m, **c.** 90 m.

units, which will then be proportional to the Chl *a* per cell. The second one (Mode 2) acts on the size of the photosynthetic unit, which will increase linearly with the increase of the Chl *a* per cell. Therefore, in our simulations, following Mode 1 P_m decreases proportionally to a decrease in θ_c whereas Mode 2 leaves P_m unaffected by any change in the per cell Chl *a* content.

Because the parameters affecting P_m are θ_c and ϑ_{Inhib}, which both depend on the irradiance experienced by the cells, the variation of P_m is significantly different in the two photoadaptative strategies. The value of P_m at steady state as a function of irradiance is significantly less affected by high irradiance in Mode 1 than in Mode 2 (Fig. 4) whereas the decrease of θ_c at high irradiance affects P_m along with the photoinhibition.

These model experiments allow the evolution of each physiological process (i.e. acclimation to mixing, light and nutrients) to be described and these govern phytoplankton growth and elucidate the physiological response times of the cells to environmental factors.

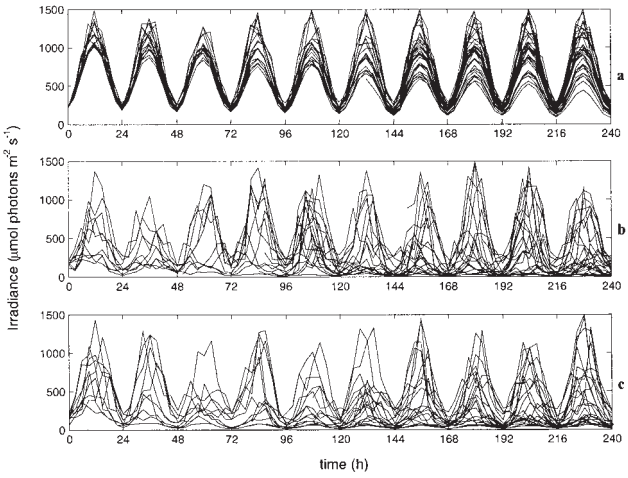

Fig. 6. The light incident upon selected particles during ten days, for three different values of the mixed layer depth: **a.** 3 m, **b.** 55 m, **c.** 90 m.

Figure 5 shows the trajectories of 25 particles for a mixed layer thickness of 3 m, 55 m and 90 m respectively, corresponding to the values measured in ice-free waters of the Ross Sea during the summer (see table I and fig. 3 in Saggiomo *et al*. 2002). According to Eq. 1 the vertical displacements of single particles clearly reflect the intensity of turbulence and thus the vertical gradient of diffusivity. The light incident upon selected particles during the time of the simulation (10 days) is shown in Fig. 6. Since the model was run under a light regime which is typical of the Antarctic summer, particles experienced irradiance levels ranging from close to 0 to slightly less than 1500 µmol photons m^{-2} s^{-1}, the upper limit of solar irradiance measured *in situ* when photosynthetic parameters were determined (Saggiomo *et al.* 2002).

Cell division (under unlimited nutrient supply condition) occurs in our model when the initial carbon cellular content

Table III. Photosynthetic parameter values used in the model.

Parameter	Value	Units
α_{Chl}	0.06	mg C·(mg Chl *a*)$^{-1}$·h^{-1} (µmol photons m^{-2} s^{-1})$^{-1}$
Q	0.2	mg N · (mg C)$^{-1}$
R^{Chl}	0.75	d^{-1}
R^{C}	0.75	d^{-1}
ζ	2.0	mg C · (mg N)$^{-1}$
σ_{PSII}	4	m^2 · (µmol photons)$^{-1}$
N	2.3×10^{-6}	mgC ·(mg Chl)$^{-1}$
τ	5	ms
k_d	0.5×10^{-7}	dimensionless
k_r	4.5×10^{-8}	ms^{-1}

https://doi.org/10.1017/S0954102004001968 Published online by Cambridge University Press

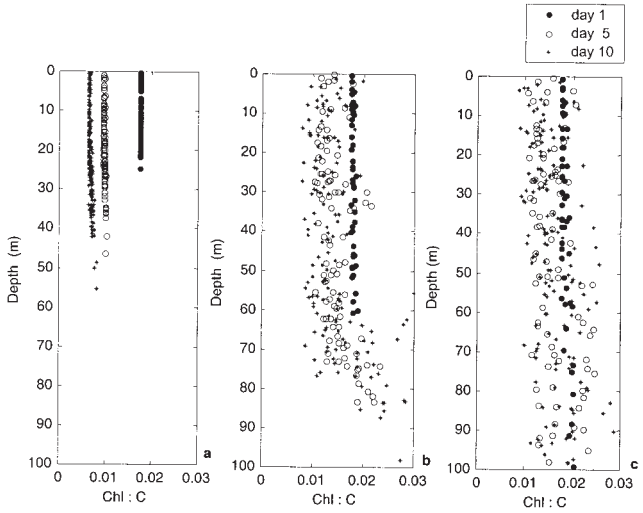

Fig. 8. The Mode1 photoacclimation history of particles in terms of the Chl : C ratio, which reflects the individual light history for different depths of the mixed layer: **a.** 3 m, **b.** 55 m, **c.** 90 m.

is doubled. The P_m values have been scaled to reproduce an average division rate of 0.3 d^{-1}, as observed in the Ross Sea in different scenarios.

The photoinhibition effect (Fig 7) has been evaluated by means of Eq. 12 using the parameter values (ϑ_{Inhib}, k_d, k_r, etc.) reported in Table III. The initial condition for the value of ϑ_{Inhib} is set to 1, assuming the absence of photoinhibition. Comparison of the results shown in Figs 5 & 7 suggests that photoinhibition is stronger (close to 0.6) when the particles are displaced in the upper few metres of the water column. Moreover, a broad range of variability in photoinhibition within the same population is revealed as the mixed layer thickness increases.

The light history of the single particles can be followed on

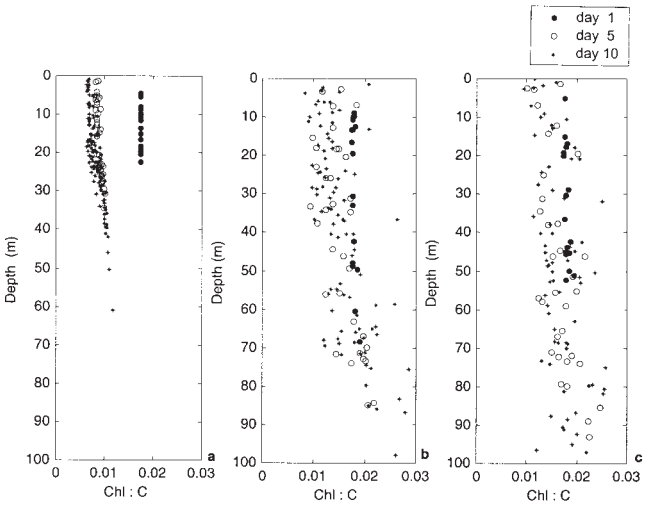

Fig. 9. The Mode 2 photoacclimation history of particles in terms of the Chl : C ratio, which reflects the individual light history for different depths of the mixed layer: **a.** 3 m, **b.** 55 m, **c.** 90 m.

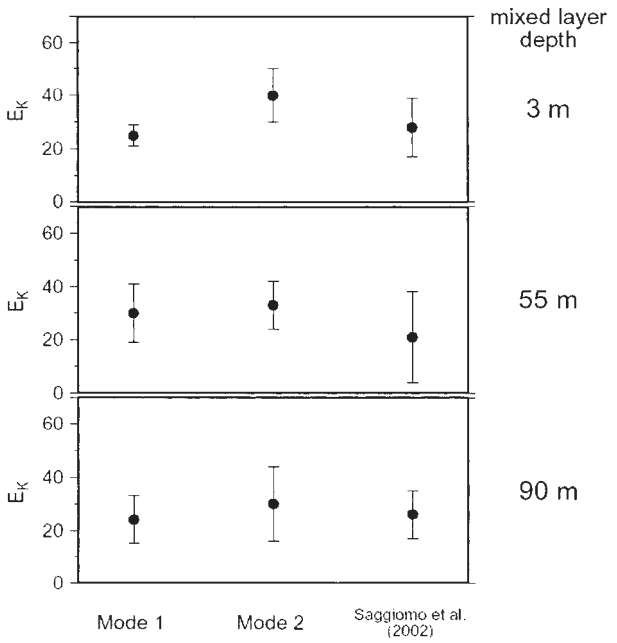

Fig. 10. Average and standard deviation of E_k (µmol photons·m^{-2}·s^{-1}) simulated (Mode 1 and Mode 2) and measured in the Ross Sea at fixed mixed layer depth.

the basis of the evolution of the Chl:C ratio, the main proxy for photoacclimation, which reflects the balance of absorbed vs utilized light. Vertical profiles of the Chl:C ratio for the selected mixed layer depths (Figs 8 & 9) refer to midday of the 1st, 5th and 10th days of simulation. This parameter, starting from 0.02 (the "ideal" Chl:C ratio), adapts towards a value reflecting the irradiance regime experienced by the single particle, and in our results ranges from 0.01 to 0.03; moreover, as the mixed layer depth increases, the population displays a wider range of ratios (Figs 8c & 9c), whereas the Chl:C ratios are quite similar for both the photoacclimation modes. From the Chl:C simulated ratios, average and standard deviation of the light saturation index E_k have been derived for each mixed layer depth as

$$E_k = \frac{P_m}{\alpha_{Chl}\theta_c}$$

(see Geider *et al.* 1997). The value range (12–60 µmol photons·m^{-2}·s^{-1}) is consistent, for both the photoacclimation modes, with *in situ* data (8–55 µmol photons·m^{-2}·s^{-1}) (Saggiomo *et al.* 2002; see Fig. 10) and underlines the role of different mixing levels in determining the light histories of the cells.

The phytoplankton biomass and primary production reflect the values of the open Ross Sea for a 0–100 m water column. Using the Mode 2 strategy, we obtained Chl *a* concentrations (Fig. 11) (between 0.02 and 1.1 mg m^{-3}) and integrated primary production values (Fig. 12) (108–629 mg C m^{-2} d^{-1}) which closely match the data in the case of 55 m mixed layer depth. The photoacclimation proxy also determines the instantaneous photosynthesis–light response

https://doi.org/10.1017/S0954102004001968 Published online by Cambridge University Press

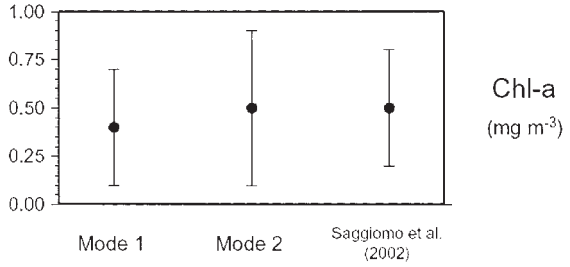

Fig. 11. Average and standard deviation of simulated and measured Chl *a* concentrations (mg m^{-3}) in the 0–100 m water column of the Ross Sea.

in terms of the carbon specific photosynthesis, which proves to be consistent with data. If we look at Fig.13 we may infer that the productivity per cell differs significantly depending on the photoacclimation strategies; in Mode1 it is lower than in Mode 2 from the surface to 55 m, but more homogeneous in the water column.

Together with the different trajectories and light histories of individual organisms, the final number of organisms after ten days of simulation differs and depends on the value of the mixed layer depth as an initial condition and the selected mode of photoacclimation. In addition, it also depends on the transparency of the water (i.e. light availability), which in turn depends on the initial concentration of chlorophyll and the presence of coloured substances dissolved in the water. The effect of the number of organisms within the population (Fig. 14a & b) has been evaluated by assuming four values for the initial concentration of the phytoplankton cells (2000, 7500, 75000, 200000 cells l^{-1}). For Mode 1 (Fig. 14a) the final number of particles ranged from 1000 particles for a 3 m mixed layer to more than 1500 for a 55 m mixed layer, being only moderately dependent on the water transparency. In contrast, cells adopting a Mode 2 strategy displayed a significantly higher growth rate and a decreasing growth rate with an increase in the mixed layer depth and a decrease in water transparency.

The Chl *a* concentration influences the available irradiance through self-shading; the latter affects the light attenuation by up to 40%. This result offers a preliminary indication of the variability of physiological responses in the phytoplankton community. As regards the photosynthetic performance, the simulations display two

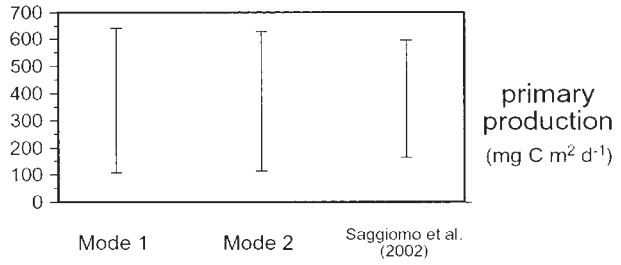

Fig. 12. Range of simulated and measured primary production (mg C m^{-2} d^{-1}) in the 0–100 m water column of the Ross Sea.

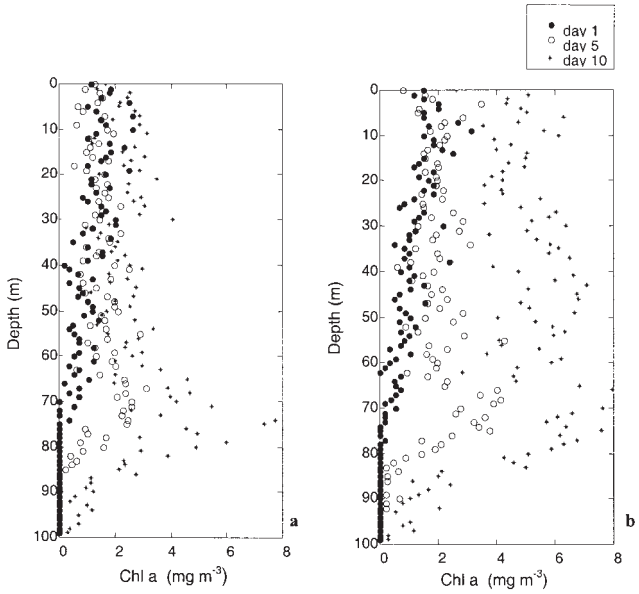

Fig. 13. Chlorophyll *a* distribution in the water column for a mixed layer depth set as 55 m. **a.** Mode 1, **b.** Mode 2.

contrasting behaviours which depend on the two modes of photoacclimation considered. As might be expected, cells that reduce the size of the photosynthetic units while keeping their number constant at decreasing Chl *a* content are less affected by high irradiance than cells which reduce the number of the photosynthetic units while maintaining their size constant. For both cell categories the photosynthetic performance is reduced by photoinhibition.

Discussion

We examined the role of different turbulent regimes and mixed layer depths on cell growth and on the depth-integrated primary production, given a set of photophysiological constraints. We also performed simulations on the basis of measured parameters and

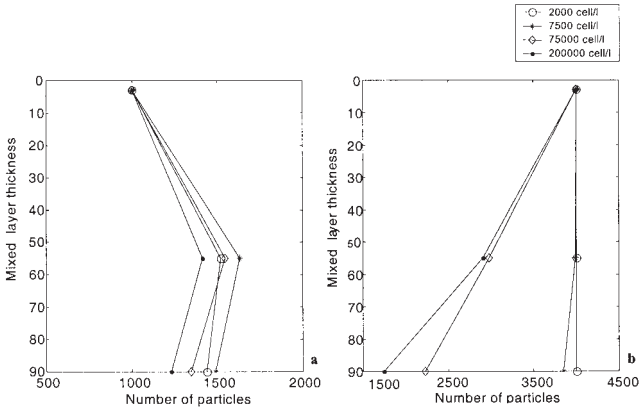

Fig. 14. The number of the particles at the end of the simulations depending on the depth of the mixed layer and on the initial concentration of cells in the water column. **a.** Mode1 **b.** Mode 2.

https://doi.org/10.1017/S0954102004001968 Published online by Cambridge University Press

realistic kinetic constants determined to be consistent with measured photosynthetic rates. The potential role of different biophysical constraints was investigated using an individual-based modelling approach. It was not our intention to generate a prognostic model of primary production in nutrient replete areas of the Southern Ocean. In addition to the novel introduction of an explicitly variable vertical diffusivity, emphasis has been given to the light history of organisms, in terms of photoacclimation, self-shading and photoinhibition. The results depend on the photoacclimation response attributed to the organisms in the model. In the case of cells which respond to an increase of irradiance by reducing the number of the photosynthetic units (Mode 1), we obtain the unexpected result that production increases with the thickness of the mixed layer to a certain threshold, reflecting the effect of the coupling of low values of the light saturation parameter (i.e. high α_{Chl} values) with significant values of β, the coefficient for photoinhibition, expressed in our parameterization by the ratio between k_d and k_r.

On the other hand, photosynthetic performance is not reduced significantly in the case of cells which respond to increasing irradiance by decreasing the size of photosynthetic unit (Mode 2), while the growth rate, which in our model is proportional to photosynthetic activity, is only slightly depressed as a result of photoinhibition. It is also partially compensated for by cell movements in the mixed layer and by the light attenuation. However, the latter also reduces photosynthesis. Therefore, at increasing cell concentrations and mixed layer thicknesses, the average irradiance available for each cell decreases, with a concurrent decrease in the final number of cells and depth integrated primary production. This means that, in a shallow mixed layer, the coupled effect of photoinhibition and photoacclimation hinders maximum productivity, whereas optimal performance is only obtained at low irradiances. In addition, the pattern still persists at high levels of light attenuation.

The productivity per cell reflects a process that is distinct from the evolution of Marginal Ice Zone blooms which develop according to the classic high nutrient-shallow mixed layer regime (Gran effect; see Mann & Lazier 1991), and reproduces a dynamic that also differs from the Sverdrup (1953) original conceptualization. In this latter paper, the relative size of the mixed layer compared to the 'critical' depth determines the net accumulation of cells. In other words, the thickness of the mixed layer favours growth, but growth reduces the mean irradiance which then becomes a decreasing function of mixed layer depth. In our results, the highest rate of cell accumulation (without mortality) is reached when the vertical mixing compensates for photoinhibition and the alternative way of responding to high irradiances - decreasing the number of photosynthetic units. Even though our results tend to exaggerate the impact of reducing the number of active photosynthetic units at high irradiance, which is partially compensated for by a parallel reduction in the turnover time (Behrenfeld *et al*. 1998), decreases in per cell carbon fixation in high vs low light regimes has been documented in several species (Geider *et al.* 1998). This response generates the maximum shown in Fig. 14a, given the assumed model for the functioning of photoacclimation-photoinhibition-photorepair system (Geider *et al.* 1998, Han *et al.* 2000). It is important to stress that a mixed layer of at least 35 m is needed to compensate for the high irradiance constraint.

According to the data, the results suggest that the low values of photosynthetic parameters (see Table I), and the related photosynthetic performance of Antarctic waters (Saggiomo *et al.* 2002), may be a response to continuous and relatively strong mixing regimes. This in turn should differentiate the photophysiological characteristics of species blooming in the Marginal Ice Zone from those living in the ice-free water (Wright and Van den Enden 2000).

In addition, minimizing the effect of photoinhibition could be a relevant selective factor in Antarctic plankton species, and the capability to resist the close-to-surface intense irradiance caused by calm weather might result in a higher growth rate.

Mode 2 simulations reproduce the Sverdrup conceptualisation with a decrease in the cell accumulation along with an increase in the thickness of the mixed layer.

Our simplified study on the potential role of mixing on the growth of phytoplankton population suggests that the interplay between light and mixing is an important controlling factor in ice-free water areas where there is no iron limitation (a crucial factor for phytoplankton growth, Martin *et al.* 1990, De Baar *et al.* 1995), but not in as simple a way as generally assumed. The work also shows the potential of Lagrangian modelling, which appears to be suitable for reconstructing the time evolution of biotic communities since they are formed by organisms whose individual history determines their physiological response to environmental factors.

Acknowledgements

The authors would like to thank Cristophe Brunet for useful discussions of the material. This work was partly funded by the CLIMA project of the Italian National Program for Antarctic Research (PNRA), the University of Siena and the Italian Space Agency.

References

Bauer, S., Swenson, M.S. & Griffa, A. 1998. Eddy-mean flow decomposition and eddy-diffusivity estimates in the tropical Pacific Ocean. *Journal of Geophysical Research*, **103**, 3855–3871.

Behrenfeld, M.J., Prasil, O., Kolber, Z.S., Babin, M. & Falkowski, P.G. 1998. Compensatory changes in Photosystem II electron turnover rates protect photosynthesis from photoinhibition. *Photosynthesis Research*, **58**, 259–268.

https://doi.org/10.1017/S0954102004001968 Published online by Cambridge University Press

Berloff, P.S. & McWilliams J.C. 2002. Material transport in oceanic gyres. Part II: Hierarchy of stochastic models. *Journal of Physical Oceanography*, **32**, 797–830.

Chandrasekhar, S. 1943. Stochastic problems in physics and astronomy. *Review of Modern Physics* **15**, 1–89.

Csanady, G.T. 1973. *Turbulent diffusion in the environment*. Dordrecht: Reidel, 248 pp.

Cullen, J.J. & Lewis, M.R. 1988. The kinetics of algal photoadaptation in the context of vertical mixing. *Journal of Plankton Research*, **10**, 1039–1063.

De Baar, H.J.W., de Jong, J.T.M., Bakker, D.C.E., Loscher, B.M., Veth, C., Bathmann, U. & Smetacek, V. 1995. Importance of iron for plankton blooms and carbon dioxide draw down in the Southern Ocean. *Nature*, **373**, 412–415.

Falkowski, P.G. & Wirick, C.D. 1981. A simulation model of the effects of vertical mixing on primary productivity. *Marine Biology*, **65**, 69–75.

Falkowski, P.G., & Raven J.A. 1997. *Aquatic photosynthesis*. Oxford: Blackwell Science, 375 pp.

Figueiras, F.G., Arbones, B. & Estrada, M. 1999. Implications of bio-optical modelling of phytoplankton photosynthesis in Antarctic waters: further evidence of no light limitation in the Bransfield Strait. *Limnology and Oceanography*, **44**, 1599–1608.

Geider, R., MacIntyre, H.L. & Kana, T.M. 1997. Dynamic model of phytoplankton growth and acclimation: responses of the balanced growth rate and the chlorophyll *a*: carbon ratio to light, nutrient-limitation and temperature. *Marine Ecology Progress Series*, **148**, 187–200.

Geider, R., MacIntyre, H.L. & Kana, T.M. 1998. A dynamic regulatory model of phytoplanktonic acclimation to light, nutrients, and temperature. *Limnology and Oceanography*, **43**, 679–694.

Griffa, A. 1996. Applications of stochastic particle models to oceanographic problems. *In* Adler, R.J., Muller, P. & Rozovskii, B.L., *eds*. *Stochastic Modelling in Physical Oceanography*. Boston, MA: Birkhauser, 113–140.

Han, B., Virtanen, M., Koponen, J. & Straskraba, M. 2000, Effect of photoinhibition on algal photosynthesis: a dynamic model. *Journal of Plankton Research*, **22**, 865–885.

Hunter, J.R., Craig, P.D. & Phillips, H.E. 1993. On the use of random walk models with spatially variable diffusivity. *Journal of Computational Physics*, **106**, 366–376.

Janowitz, G.S. & Kamykowski, D. 1999. An expanded Eulerian model of phytoplankton environmental response. *Ecological Modelling*, **118**, 237–247.

Lande, R. & Lewis, M.R. 1989. Models of photoadaptation and photosynthesis by algal cells in a turbulent mixed layer. *Deep-Sea Research*, **36**, 1161–1175.

Lazzara, L., Saggiomo, V., Innamorati, M., Mangoni, O., Massi, L., Mori, G. & Nuccio, C. 2000. Photosynthetic parameters, irradiance, biooptical properties and production estimates in the Western Ross Sea. *In* Faranda, F.M., Guglielmo, L. & Ianora, A., *eds*. *Ross Sea ecology*. Berlin: Springer, 259–273.

Lizon, F., Seuront, L. & Lagadeuc, Y. 1998. Photoadaptation and primary production study in tidally mixed coastal waters using a Lagrangian model. *Marine Ecology Progress Series*, **169**, 43–54.

Mann, K.H. & Lazier, J.R.N. 1991. *Dynamics of marine ecosystems*: *biological physical interactions in the oceans*. Boston: Blackwell Scientific, 466 pp.

Marra, J. 1978. Effect of short-term variations in light intensity on photosynthesis of a marine phytoplankter: a laboratory simulation study. *Marine Biology*, **46**, 191–202.

Marshall, H.L., Geider, R.J. & Flynn, K.J. 1999. A mechanistic model of photoinhibition. *New Phytology*, **145**, 347–359.

Martin, J.H., Fitzwater, S.E. & Gordon R.M. 1990. Iron deficiency limits phytoplankton growth in Antarctic waters. *Global Biogeochemical Cycles*, **4**, 5–12.

Mortain-Bertrand, A. 1989. Effects of light fluctuations on the growth and productivity of Antarctic Diatom in Culture. *Polar Biology*, **9**, 245–252.

Nelson, D.M. & Smith Jr, W.O. 1991. Sverdrup revisited: critical depths, maximum chlorophyll levels, and the control of Southern Ocean productivity by the irradiance-mixing regime. *Limnology and Oceanography*, **36**, 1650–1661.

Neori, A. & Holm-Hansen, O. 1982. Effect of temperature on rate of photosynthesis in Antarctic phytoplankton. *Polar Biology*, **16**, 1–11.

Saggiomo, V., Carrada, G.C., Mangoni, O., Marino, D. & Ribera d'Alcala' M. 2000. Ecological and physiological aspects of primary production in the Ross Sea. *In* Faranda, M., Guglielmo, L. & Ianora, A., *eds*. *Ross Sea ecology*. Berlin: Springer, 247–258.

Saggiomo, V., Catalano, G., Mangoni, O., Budillon, G. & Carrada, G.C. 2002. Primary production processes in ice-free waters of the Ross Sea (Antarctica) during the austral summer 1996. *Deep Sea Research II*, **49**, 1787–1801.

Sakshaug, E. & Holm-Hansen O. 1986. Photoadaptation in Antarctic phytoplankton: variations in growth rate, chemical composition and P versus I curves. *Journal of Plankton Research*, **8**, 459–473.

Sakshaug, E., Slagstad, D. & Holm-Hansen, O. 1991. Factors controlling the development of phytoplankton blooms in the Antarctic Ocean – a mathematical model. *Marine Chemistry*, **35**, 259–271.

Sakshaug, E., Bricaud, A., Dandonneau, Y., Falkowski, P.G., Kiefer, D.A., Legendre, L., Morel, A., Parslow, J. & Takahashi, M. 1997. Parameters of photosynthesis: definitions, theory and interpretation of results. *Journal of Plankton Research*, **19**, 1637–1670.

Strutton, P.G., Griffiths, F.B., Waters, R.L., Wright, S.W. & Bindoff, N.L. 2000. Primary productivity off the coast of East Antarctica (80–150°E): January to March 1996. *Deep Sea Research II*, **47**, 2327–2362.

Sverdrup, H.U. 1953. On conditions of the vernal bloom of phytoplankton. *Journal du Conseil International pour l'Exploration de la Mer*, **18**, 287–295.

Thomson, D.J. 1987. Criteria for the selection of stochastic models of particle trajectories in turbulent flows. *Journal of Fluid Mechanics*, **180**, 529–556.

Tilzer, M.M. & Dubinsky, Z. 1987. Effect of temperature and day length on the mass balance of Antarctic phytoplankton. *Polar Biology*, **7,** 35–42.

van Dop, H., Niewstadt, F.T.M. & Hunt, J.C.R. 1985. Random walk models for particle displacements in inhomogeneous unsteady turbulent flows. *Physics of Fluids*, **28**, 1639–1653.

Visser, A.W. 1997. Using random walk models to simulate the vertical distribution of particles in a turbulent water column. *Marine Ecology Progress Series*, **158**, 275–281.

Wolf, K.U. & Woods, J.D. 1988. Lagrangian simulation of primary production in the physical environment - the deep chlorophyll maximum and nutricline. *In* Rothschild, B.J., *ed*. *Toward a theory on biological-physical interactions in the world ocean.* Dordrecht: Kluwer, 51–70.

Woods, J. & Onken, R. 1982. Diurnal variation and primary production in the ocean: preliminary results of a Lagrangian ensemble model. *Journal of Plankton Research*, **4**, 735–756.

Wright, S.W. & van den Enden, R.L. 2000. Phytoplankton community structure and stocks in the East Antarctic marginal ice zone (BROKE survey, January–March 1996) determined by CHEMTAX analysis of HPLC pigment signatures. *Deep Sea Research II*, **47**, 2363–2400.

Yamazaki, H. & Kamykowski, D. 1990. The vertical trajectories of motile phytoplankton in a wind-mixed water column. *Deep-Sea Research*, **38**, 219–241.

Young, W.R., Roberts, A.J. & Stuhne, G. 2001. Reproductive pair correlations and the clustering of organisms. *Nature*, **412**, 328–331.

Zambianchi, E. & Griffa, A. 1994. Effects of finite scales of turbulence on dispersion estimates, *Journal of Marine Research*, **52**, 129–148.